High Frequency Mode Cascades in the ASDEX Upgrade Tokamak

K. Hallatschek, A. Gude, D. Biskamp, S. Günter, and the ASDEX Upgrade Team
Max-Planck Institut für Plasmaphysik, EURATOM-IPP Association, D-85748 Garching, Germany
(Received 2 September 1997)

Using a novel diagnostic, cascades of high frequency modes have been observed in the core plasma of the ASDEX Upgrade tokamak. Their mode numbers obey the relation $m = n + 1$, with n up to 23. The appearance of cascades is always related to a region of low shear, which is ascribed to previous $(m, n) = (1, 1)$ mode activity and leads to the instability of tearing modes with high mode numbers. The destabilization and stabilization of modes resulting in the cascade process can be reproduced by a simple quasilinear model. [S0031-9007(97)04968-5]

PACS numbers: 52.55.Fa, 52.30.Jb, 52.35.Py, 52.70.La

In all tokamaks, coherent oscillations of the poloidal magnetic field have been measured by Mirnov coils. These usually are unstable tearing modes with mode numbers up to $m \sim n \sim 5$ [1]. Higher mode numbers (6–15) have been observed, mostly by means of microwave reflectometry and electron cyclotron emission measurements [2], or soft x-ray (SXR) measurements [3] because of the fast radial decay of their field perturbations. High-n modes are conventionally identified with pressure driven instabilities such as ballooning modes. On ASDEX Upgrade, a wavelet-transform-based, real-time algorithm for the detection of plasma events has been applied to the SXR signals [4]. During a discharge, the data acquisition system automatically chooses a sampling rate which is adequate to the detected plasma events. With this novel technique, modes with high mode numbers ($m, n \sim 20$) have been observed in the core plasma of ASDEX Upgrade by the SXR diagnostics during transient states of certain discharges. The modes are excited by a peculiar mechanism: Each mode with mode numbers $(m, n) = (n + 1, n)$ triggers its successor, with m, n increased by one, and is stabilized again. Via a domino effect, initial modes with $m, n \sim 5$ excite cascades progressing up to high mode numbers. Despite the high mode numbers, these modes can be understood by a simple model based on tearing modes. Because of the transient nature (50 ms) of the cascades, their observation is improbable without the use of a real-time event detection technique for the data selection.

Experimental observations.—The cascades are most easily recognized in the time-dependent frequency spectra of the SXR signals, since the plasma rotation permits the distinguishing of modes with different mode numbers by their frequency differences. Figure 1(a) shows cascades with clearly visible frequency rise due to the excitation of successively higher mode numbers, whereas the slower cascades in Fig. 1(b) exhibit well-separated discrete mode frequencies, showing that a cascade is not a single chirplike event.

Analysis of the SXR data has shown that the mode numbers in a cascade can be described by $m = n + 1$, each mode being followed by one with mode numbers raised by one. Cascades start typically with $n \sim 5$ and can progress up to $n \sim 23$, corresponding to frequencies of $\sim$210 kHz. The maximum attained mode numbers decrease with time until cascading stops and the $(4, 3)$ and $(3, 2)$ become the only active modes. The mode radii and the q profiles (Fig. 2) have also been inferred from SXR data, assuming that a mode (m, n) is located at a flux surface with

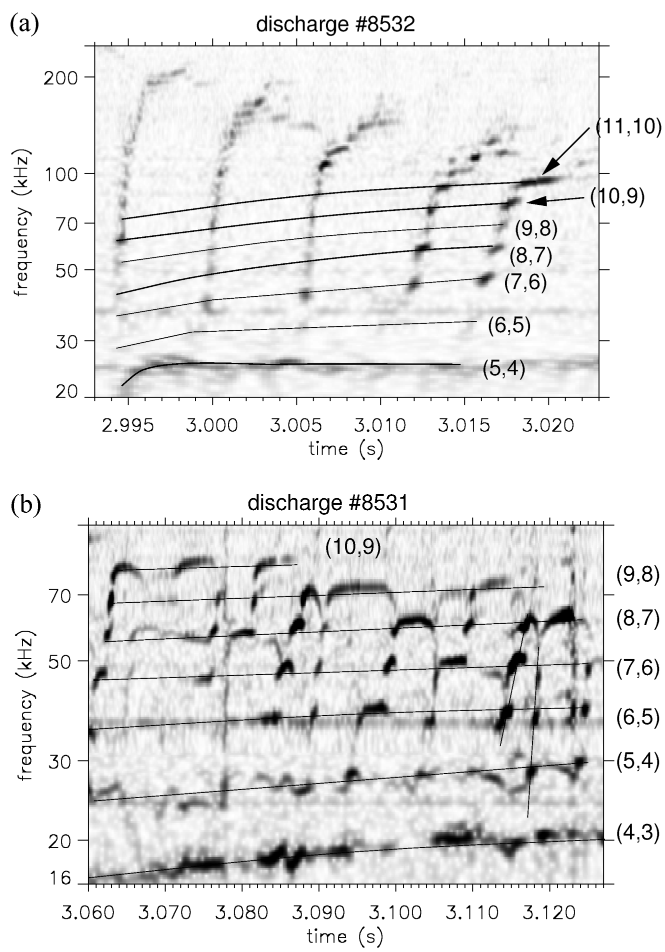

FIG. 1. Gray scale plots of the wavelet transform of signals of a central SXR chord.

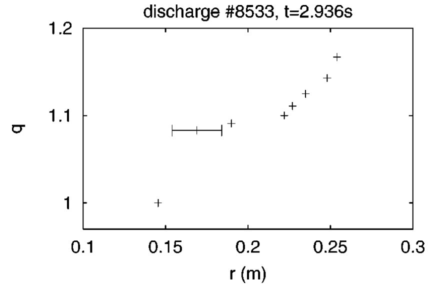

FIG. 2. Typical q profile during cascades.

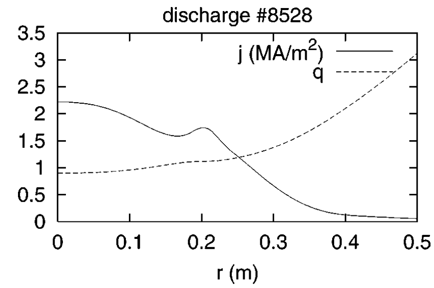

FIG. 3. Experimental q and j profiles.

$q = m/n$. Most cascades propagate inward, corresponding to positive shear. In some discharges, outward propagating cascades, presumably corresponding to negative shear, have been observed, though for these cascades the mode radii were too small to allow the determination of the q profile. The modes are accompanied by radial shifts of the SXR emissivity profile analogous to sawteeth.

The given poloidal mode numbers for $m \leq 7$ are based on the relative phases and amplitudes of the oscillations observed by two SXR pinhole cameras (eight relevant chords per camera) [5]. The toroidal mode number of the (3,2) and (4,3) modes has been determined from the phase differences obtained from five toroidally displaced Mirnov coils. The higher n numbers have been concluded from the fact that the frequency is always increased by 7–12 kHz, which coincides with what is expected from the ion toroidal rotation for an n increment of one (10 ± 3 kHz). The frequency difference due to the m increase and the ion/electron diamagnetic drift is $\sim$2 kHz and therefore negligible. The ion toroidal rotation was measured by the Doppler shift in charge exchange recombination lines. The temperature and density profiles have been obtained from Thomson scattering and interferometer data. If the increment in m from one mode to the next was not one for an $m > 7$, the q profiles would exhibit an unphysical jump, since the helicity difference between, e.g., an $(m + 2, m)$ and an $(m, m - 1)$ is $\delta q \sim 1/n$, which is much larger than the regular change $\delta q \sim 1/n^2$ between an $(m + 1, m)$ and an $(m, m - 1)$. The mode radii have been inferred from observations of the oscillations (for $m \leq 12$) and the shift of SXR emissivity.

The q profiles exhibit a shoulder with very low shear ($d \ln q / d \ln r \sim 0.004$–$0.1$), which can be resolved reliably by the SXR diagnostics because of the very small q-differences of the modes. The shoulder in q leads to a peak in the toroidal current-density profiles calculated from interpolated q profiles in cylindrical approximation (Fig. 3).

The mode frequencies can be explained within measurement errors by toroidal plasma rotation and diamagnetic drifts. For example, the fast frequency rise (fall) during the growth of a mode in discharges with coinjection (counterinjection) can be attributed to the change in diamagnetic rotation frequency due to a reduction of the pressure gradient at the mode position.

Prior to the cascades, a $(1,1)$ internal kink mode is observed, which attenuates and whose radius decreases, indicating a contraction of the $q = 1$ surface. Its initial radius coincides with the average radius of the cascade modes. The contraction is a result of an increase in central plasma resistivity (Fig. 4) caused by impurity accumulation, which occurs essentially unpredictably in some discharges.

The scenario described has been observed under various plasma conditions such as coinjection and counterinjection, β_p from 0.6 to 0.8, neutral-beam heating powers from 2 to 7.7 MW, and ion-cyclotron-resonance heating powers from 0 to 1 MW.

Stability of high-(m, n) modes.—The usual candidates for high-(m, n) mode activity, ballooning modes, are stable because of the moderate pressure gradients at the position of the cascading modes [7]. In principle, resistive interchange modes have to be taken into consideration because of the just marginally favorable field line curvature $\kappa_n = \kappa_c(1 - q^2) \ll \kappa_c$ [8] which is modified by the noncircular cross section of the ASDEX Upgrade plasma. However, in these cases, interchange modes are well stabilized by the plasma compressibility in conjunction with the anomalous viscosity [9].

The instability of tearing modes with high mode numbers can be understood by the following simple

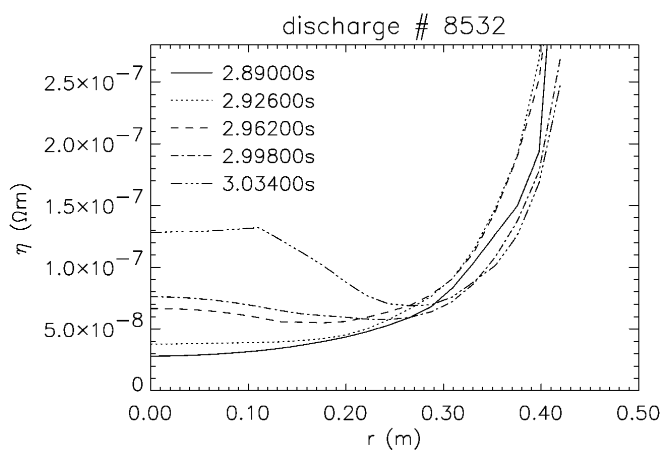

FIG. 4. η profile [6] preceding the cascades. The onset of the cascades was at 2.96 s.

consideration. In the cylindrical tearing mode equation,

$$\frac{d^2\psi}{dr^2} + \frac{1}{r}\frac{d\psi}{dr} - \left(\frac{m^2}{r^2} + \frac{qRdj/dr}{B_z r[1 - nq(r)/m]}\right)\psi = 0\,, \tag{1}$$

we replace ψ by $\sqrt{r}\,\hat{\psi}$ and expand the coefficients around the singular surface r_s, assuming that the perturbed flux is localized there, which yields

$$\frac{d^2\hat{\psi}}{dx^2} - \left(1 + \frac{\alpha}{x}\right)\hat{\psi} = 0 \tag{2}$$

with the abbreviations $x = k(r - r_s), k \approx m/r_s, \alpha \approx r_s q''/nq'$ for $q'' \gg 3q'/r_s, q'' \gg 2q'^2, m = n + 1, n \gg 1$. With the appropriate boundary conditions ($\hat{\psi} \to 0$ for $x \to \pm\infty$, $\hat{\psi}$ continuous at r_s) this equation can be solved analytically and the stability parameter $\Delta' = [\psi'(r_s + \epsilon) - \psi'(r_s - \epsilon)]/\psi(r_s)$ can be obtained. Instability is expected if $\Delta' > 0$, or in this approximation if

$$\alpha > 1\,. \tag{3}$$

Estimating α by finite-differencing measured q profiles results in instability of the cascading modes because of the combined effect of the low shear and the kink in the q profiles (at $r = 0.23$ m and $r = 0.25$ m in Figs. 2 and 3).

The predictions of this rather crude estimate are supported by numerical stability analysis of spline fits of the observed q profiles. (Because of the sensitivity of the effect to small profile changes, the results depend somewhat on the specific way the fit is obtained.) Also the stability analysis of the full MHD equations for ASDEX Upgrade equilibria, based on the measured q profiles and using the code CASTOR, yields unstable modified tearing modes with growth rates depending also on the pressure gradient [10].

Cascading mechanism.—In a cascade a mode (m, n) destabilizes its successor $(m + 1, n + 1)$ and stabilizes its predecessor $(m - 1, n - 1)$. Toroidal coupling of different modes can be ruled out, because of the different toroidal mode numbers. Also nonlinear mode coupling effects are weak since the (1,1) mode is usually absent. Therefore the most probable cause for mode growth or decay is changes of the equilibrium profiles.

To model a cascading mechanism based on the change of the current profile, the reduced cylindrical MHD equations [11] have been solved in the quasilinear approximation. Dissipation was assumed to be governed by resistivity, neglecting, e.g., electron viscosity.

The mutual effects of two successive modes [e.g., (7,6) and (8,7)] have been studied for a measured q profile. It has been found that the saturated amplitude of the single helicity state of the successor mode is increased by the presence of the predecessor mode, added with a small amplitude and soon growing to saturation, which indicates the destabilizing effect on the successor mode. On the other hand, the addition of the successor mode to a single helicity saturated state of the predecessor has a strong stabilizing effect on the latter. These processes, the quasilinear destabilization of the successor by the predecessor and the stabilization of the latter by the former, are the basic ingredients of the mode number increase in the cascade process.

Both effects can lead to multiple cascades, as shown in Fig. 5, if an appropriate model current profile is used. The resulting space averaged amplitudes of the perturbed helical flux in Fig. 5(a) exhibit maxima running from low to high mode numbers, similar to the experimental findings in Fig. 1. The corresponding equilibrium current profiles during the second cascade in Fig. 5(b) show a current-density plateau, which propagates inward simultaneously with the excitation of the corresponding modes. The simulated cascades even exhibit some of the irregular behavior of Fig. 1(b), in that the (12,11) and the (13,12) don't always appear.

Starting from the realistic measured profiles, the quasilinear model results in only one cascade leaving the modes at stationary finite amplitudes. To make the cascade process repetitive, as observed experimentally, an additional process is needed, which switches the modes on

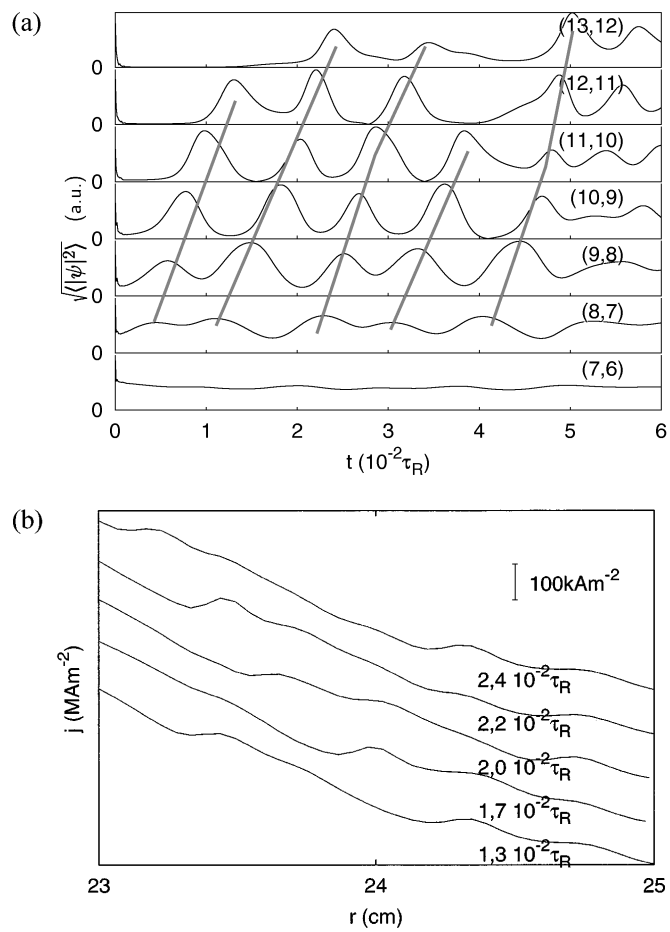

FIG. 5. Simulation using a model current profile. (a) Space averaged amplitudes of flux perturbations; (b) (0,0) current-density profile vertically displaced at different times.

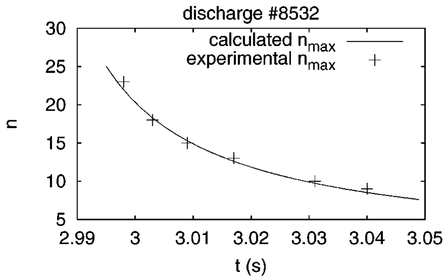

FIG. 6. Calculated and experimental mode numbers attained by the cascades of Fig. 1.

and off more efficiently, when the stability threshold is crossed. For example, the braiding of field lines due to overlapping magnetic islands of successive modes giving rise to enhanced hyperresistivity [12,13], the finite ratio of perpendicular and parallel heat conductivities [14] or the finite ion Larmor radius [15], might provide such switching.

For slightly reversed shear in the flattened region, an analogous model can be applied on the inner edge of the q plateau resulting in outward progressing cascades, as were also observed in some discharges of ASDEX Upgrade.

Setup of the low shear region and onset of the cascade process.—As mentioned, the mode cascades are always preceded by a (1,1) mode, whose radius contracts due to the abruptly increased central resistivity. The mode is theoretically expected and experimentally [16] known to flatten the q profile at the $q = 1$ surface, which gives rise to an increased current gradient just outside the flat region. After the impurity accumulation, the q evolution in the low shear region is determined by current diffusion,

$$\dot{I} = 2\pi r \frac{d}{dr}[\eta(r)j(r)] = 2\pi r j \eta'(r)\,. \qquad (4)$$

$$q = \frac{2\pi B_z r^2}{I(r)R}, \qquad I(r) = \int_0^r 2\pi r' j(r')\,dr', \qquad (5)$$

where use has been made of $q \approx \text{const} \Rightarrow j' \approx 0$ in the low shear region. Consequently, only a hollow resistivity profile exhibiting a negative η gradient (Fig. 4) can result in a rise in q above one in the flattened region, causing resonant surfaces with $m/n > 1$ to move into the region of low shear.

The mode numbers are limited by the diffusive broadening of the kink in q, the range of q in the flattened region and the increase of the minimum q' caused by nonuniform η' as determined by (4). Unfortunately, a comparison of the latter effects with experimental results is not possible due to the unknown η gradient. Considering an idealized flat q at $q = 1$ and, correspondingly, a steplike initial current distribution, the diffusive broadening of the outer edge of the flat region can be analytically described. Assuming that a mode shifts a current gradient from one resonant surface to the next, the maximum poloidal mode number, destabilized by the domino effect, can be estimated by criterion (3). The result depends on the radius of the resonant surface r, the radius r_0 of the former $(1,1)$, which flattened q by partial reconnection, the plasma resistivity η, and (weakly through a cube root) the current step height δj. This estimate agrees very well with the experimentally attained mode numbers (Fig. 6) using the experimental values and assuming a reasonable δj.

In summary, using real-time event detection on the SXR diagnostics, cascades of high frequency modes have been observed as a transient event in the core plasma of the ASDEX Upgrade tokamak, with mode numbers $(n + 1, n)$, where n progresses up to 23. During the cascades, the q profile exhibits a plateau region in the helicity range of the cascade modes. The probable cause of the plateau are (1,1) mode activity and impurity accumulation, which are always observed prior to the cascades. Contrary to conventional wisdom, which restricts tearing instabilities to low mode numbers, these modes can be interpreted as tearing modes destabilized by the q plateau. A quasilinear simulation of the reduced cylindrical MHD equations can reproduce the cascade process. Because of the small helicity differences, the cascading modes can, in principle, be used as a diagnostic tool for the measurement of the q profile in regions of low shear.

The authors would like to thank Dr. R. Wolf for valuable discussions.

[1] Z. Chang *et al.*, Phys. Rev. Lett. **74**, 4663 (1995).
[2] R. Nazikian *et al.*, Phys. Plasmas **3**, 593 (1996).
[3] S. Sesnic *et al.*, Nucl. Fusion **33**, 1877 (1993).
[4] K. Hallatschek *et al.* (to be published).
[5] M. Bessenrodt-Weberpals *et al.*, Plasma Phys. Control. Fusion **38**, 1543 (1996).
[6] L. Spitzer, *Physics of Fully Ionized Gases* (Interscience, New York, 1960).
[7] G. Bateman and D. B. Nelson, Phys. Rev. Lett. **41**, 1804 (1978).
[8] V. D. Shafranov and E. I. Yurchenko, Sov. Phys. JETP **38**, 283 (1974).
[9] R. Fitzpatrick, "Stability of Coupled Tearing and Twisting Modes in Tokamaks," Institute for Fusion Studies Report No. 649, University of Texas, 1994.
[10] S. Günter *et al.* (to be published).
[11] See, e.g., D. Biskamp, *Nonlinear Magnetohydrodynamics* (Cambridge University Press, Cambridge, England, 1993), p. 17.
[12] P.K. Kaw and E.J. Valeo, Phys. Rev. Lett. **43**, 1398 (1979).
[13] R. B. White *et al.*, Phys. Fluids B **1**, 977 (1989).
[14] R. Fitzpatrick, Phys. Plasmas **2**, 825 (1995).
[15] A. I. Smolyakov *et al.*, Plasma Phys. Control. Fusion **35**, 657 (1993).
[16] R. D. Gill *et al.*, Nucl. Fusion **29**, 821 (1989).